

# An LNA With Optimally Mismatched Antenna Interface for Energy Harvesting Sensor Nodes

Yao Liu and Wouter A. Serdijn

Biomedical Electronics Group, Delft University of Technology, the Netherlands

Email: y.liu-2@tudelft.nl and w.a.serdijn@tudelft.nl

**Abstract**— In order to dramatically reduce the size of energy harvesting sensor nodes, it's necessary for a receiver to share the same antenna with an energy harvester. However, the standard  $50\Omega$  power matched interface is only designed for the connection of the antenna and the LNA, rather than taking into account the presence of the energy harvester. This paper presents an optimally mismatched antenna interface and an LNA based on this interface for the combination of the energy harvester and the LNA. The interface offers large passive voltage boosting to improve the voltage gain and NF of the LNA in a low power environment, and increases the sensitivity of the energy harvester as well. The interface and LNA have been designed and verified with simulations in AMS 0.18 $\mu\text{m}$  technology. A comparison with another LNA design based on a standard  $50\Omega$  power matched interface shows the proposed LNA has 12.3dB higher voltage gain and 1.8dB lower NF at a power consumption of  $50\mu\text{W}$ .

## I. INTRODUCTION

Energy harvesting sensor nodes (EHSNs) have gained more and more interest in wireless sensor network (WSN) and wireless body area network (WBAN) applications. Besides a data link, these sensor nodes also have a wireless energy link enabled by an RF energy harvester. Nowadays, energy link [1], [2] and data link [3], [4] are mainly optimized separately. Only a few papers discuss their system level integration [5]. In these systems, the two links are effectively decoupled by employing two different frequency bands, but demanding two bulky antennas and associated external matching components, thereby limiting the size reduction of the whole sensor node.

Sharing the same antenna between an energy link and a data link, as shown in Fig. 1, is necessary to reduce the size of an EHSN dramatically, but presents some design challenges at the antenna interface. Since the energy harvester and receiver operate concurrently most of the time, the challenges to be addressed mainly stem from the energy harvester and receiver, while the transmitter can be easily isolated from them. Thus, careful attention is required to the interface of the antenna, energy harvester and the first active stage of the receiver, i.e., the LNA.

The antenna interface of an energy harvester is usually optimized to increase the available input voltage by a voltage-boosting network [1], [2]. This is realized by combining the inductive behavior of a high-Q loop antenna with the capacitive input impedance of the rectifier. However, an LNA interface is usually designed for a  $50\Omega$  resistive input impedance, which is not optimized for a high-Q inductive antenna and will reduce the passive gain of voltage-boosting network considerably.

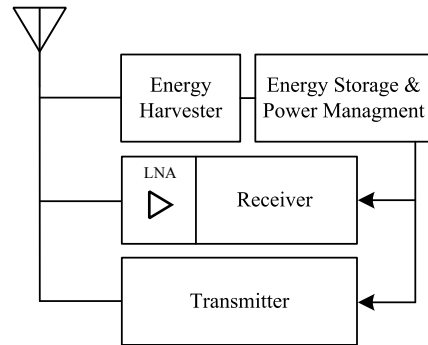


Fig. 1: System overview of the EHSN.

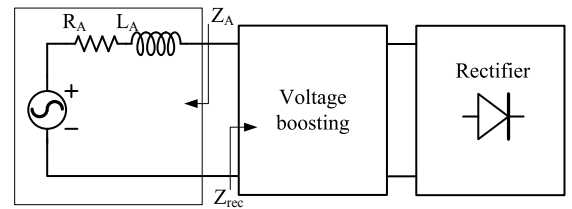


Fig. 2: Voltage-boosting energy harvester interface [1].

Moreover, a  $50\Omega$  impedance requirement adds an important constraint on the LNA design and makes designers lose two degrees of freedom, i.e., the selection of the antenna and antenna interface, thereby restricting the performance and power reduction of the LNA. Taking into account the extremely limited power budget, this limitation is more severe in EHSN applications.

In this paper, an optimally mismatched (OM) antenna interface for the combination of the energy harvester and the LNA, and an LNA based on this interface are presented. In section II, an antenna interface analysis is given. The circuit design of the LNA is discussed in Section III and verified with simulation results in Section IV. Finally, this paper ends with the conclusions.

## II. ANTENNA INTERFACES

### A. RF Energy Harvester Interface

An effective energy harvester interface is depicted in Fig. 2 [1]. In contrast to the conjugate matched antenna interface, the antenna load impedance  $Z_{rec}$  is designed to be purely capacitive, i.e.  $\text{Re}(Z_{rec}) = 0$  and  $\text{Im}(Z_{rec}) = -\text{Im}(Z_A)$ , yielding a large voltage gain, thus reducing the minimally

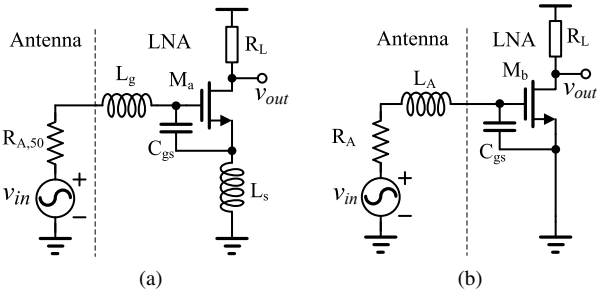


Fig. 3: (a) 50 $\Omega$  PM antenna-LNA interface (b) OM antenna-LNA interface.

required input power level for a fixed turn-on voltage rectifier. The voltage gain is  $G_{V,boost} = X_{LA}/R_A$ , where  $X_{LA}$  and  $R_A$  are the impedance of antenna inductance and resistance, respectively. It shows that  $G_{V,boost}$  can be increased by decreasing  $R_A$ . Hence, a high Q inductive antenna is preferred in this interface instead of a standard 50 $\Omega$  antenna. In order to avoid standing wave phenomena, the high Q inductive antenna is directly connected to the energy harvester.

#### B. 50 $\Omega$ Power Matched (PM) Antenna-LNA Interface

In the absence of the energy harvester, the design of LNA very often starts with the requirement of a 50 $\Omega$  input impedance. Consider an usual interface with a 50 $\Omega$  antenna, a 50 $\Omega$  band select filter and an LNA connected in series. The first reason for 50 $\Omega$  power matching is that any deviation from the desired 50 $\Omega$  load impedance of the antenna and the filter may significantly affect the passband and stopband characteristics of the filter, or produce uncharacterized loss at the antenna-LNA interface [6]. Secondly, the antenna, band select filter and LNA are usually connected by means of 50 $\Omega$  transmission lines, making the distance between the antenna signal and the LNA comparable with the wavelength at high frequencies. The interfaces may suffer from significant reflections due to the standing wave phenomena if the input/output impedance deviates from 50 $\Omega$  [6].

Assume an LNA is added to the interface shown in Fig. 2 by being directly connected to the antenna. In contrast to the 50 $\Omega$  antenna of the usual interface shown above, the high Q inductive antenna in this interface doesn't have a 50 $\Omega$  impedance, and it is directly connected to the circuitry, without any filter and transmission lines. Moreover, the distance between the antenna signal and the LNA is short enough to neglect the standing wave phenomena at the frequency of interest (915MHz). Thus, 50 $\Omega$  power matching is not a requirement for this compact interface with the inductive antenna directly connected to the LNA at 915MHz.

Let us now check the effect of 50 $\Omega$  power matching on the principal design targets of an LNA, viz gain and noise figure (NF). Considering a common source (CS) inductively source degenerated LNA as shown in Fig. 3a, a 50 $\Omega$  input resistance is created with the aid of a source inductance  $L_s$ , a gate inductance  $L_g$  and a parasitic gate capacitance  $C_{gs}$ .

The input impedance is  $Z_{in,LNA,a} = R_{A,50} = 50\Omega$ . In LNA design, voltage gain is more meaningful than power gain as the intrinsic input quantity to a transistor gate is a voltage. The voltage gain from the antenna signal  $v_{in}$  to the output voltage  $v_{out}$  at the resonance is given by

$$G_{PM} = \frac{v_{out}}{v_{in}} = Q_{in,PM} g_m R_L = \frac{X_{Lt}}{2R_{A,50}} g_m R_L \quad (1)$$

where  $g_m$  is the transconductance of  $M_a$ ,  $Q_{in,PM}$  is the passive voltage gain at the interface,  $X_{Lt} = X_{Lg} + X_{Ls}$  is the total impedance of  $L_g$  and  $L_s$ , and  $R_L$  is the load resistance at the resonance frequency.

We now determine the NF. The total output noise current is contributed by the channel noise of the transistor  $i_{nd}^2 = 4kT\gamma g_m \Delta f$ , load noise  $i_L^2 = 4kT\Delta f/R_{Ln}$ , and the thermal noise of the antenna resistance  $v_{n,R_{A,50}}^2 = 4kTR_{A,50}\Delta f$  multiplied by the effective transconductance  $Q_{in,PM}g_m$ .  $\gamma$  is a parameter often between  $\frac{1}{2}$  and 1,  $k$  is Boltzmann's constant,  $T$  is the absolute temperature,  $\Delta f$  is the bandwidth, and  $R_{Ln}$  is the equivalent noise resistance of the load, respectively. Thus

$$NF_{PM} = 1 + \frac{R_{A,50}}{X_{Lt}^2} \left( \frac{\gamma}{g_m} + \frac{4}{g_m^2 R_{Ln}} \right) \quad (2)$$

Eq. (1) and (2) show that the voltage gain and NF can be improved by increasing  $X_{Lt}$  or decreasing antenna resistance  $R_{A,50}$  when  $g_m$  and the load are given, but unfortunately,  $R_{A,50}$  is fixed by the 50 $\Omega$  power matching requirement, leaving only one degree of freedom in the antenna interface design, being to increase  $X_{Lt}$ .

The above analysis suggests that an interface is not obliged to satisfy a 50 $\Omega$  power matching requirement when a high Q inductive antenna is directly connected to an LNA at the frequency of interest (915MHz). Moreover, such a 50 $\Omega$  requirement also limits voltage gain and NF. Taking into account the energy harvester, the input resistance of a 50 $\Omega$  PM LNA will reduce the voltage-boosting gain considerably.

#### C. OM Interface

The combination of energy harvester and LNA will introduce more design constraints than the separated optimization of the energy harvester or the LNA, demanding more degrees of freedom to improve the overall performance. The observations in section II-B indicate that the 50 $\Omega$  power matching constraint can be released.

An OM interface as shown in Fig. 4 is proposed. The LNA shares the same high Q inductive antenna and voltage-boosting network with the rectifier. Instead of being 50 $\Omega$ ,  $Z_{rec}$  is designed to be purely capacitive, thus not affecting the voltage gain of the voltage-boosting network at all and improving the gain and NF of the LNA as shown soon.

Fig. 3b is a CS LNA with the proposed OM antenna interface. The input impedance of the LNA  $Z_{in,LNA,OM} = -jX_{LA}$ . Assume  $M_b$  has the same size ( $C_{gs}$ ) and transconductance  $g_m$  as  $M_a$ , and antenna inductance  $L_A$  is the same as  $L_t = L_g + L_s$  in Fig. 3a. The voltage gain then becomes

$$G_{OM} = \frac{X_{LA}}{R_A} g_m R_L \quad (3)$$

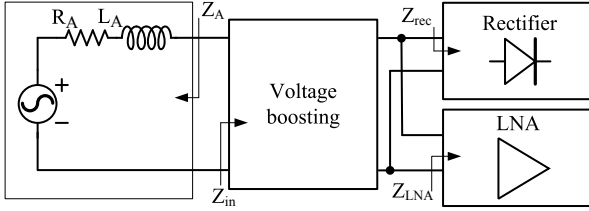


Fig. 4: Proposed OM interface.

The ratio of  $G_{PM}$  and  $G_{OM}$  is

$$\frac{G_{OM}}{G_{PM}} = \frac{2R_{A,50}}{R_A} \quad (4)$$

The NF of an OM LNA equals

$$NF_{OM} = 1 + \frac{R_A}{X_{L_A}^2} \left( \frac{\gamma}{g_m} + \frac{1}{g_m^2 R_{Ln}} \right) \quad (5)$$

And hence we have the ratio of  $NF_{PM} - 1$  and  $NF_{OM} - 1$

$$\frac{NF_{OM} - 1}{NF_{PM} - 1} = \frac{R_A}{R_{A,50}} \frac{g_m R_{Ln} \gamma + 1}{g_m R_{Ln} \gamma + 4} \quad (6)$$

Eq. (3) and (5) show that one extra degree of freedom, i.e.  $R_A$ , is gained from the proposed OM interface. In contrast to the  $50\Omega$  PM interface, a higher voltage gain and a lower NF can be achieved by choosing a small  $R_A$ , as indicated by Eq. (4) and (6). These benefits are particularly advantageous to the LNA in EHSNs due to their extremely limited power budget.

### III. CIRCUIT DESIGN

#### A. LNA

An LNA with the proposed OM interface is shown in Fig. 5. The LNA is in differential form since it's compatible with the differential rectifier to be shown later in this section. Moreover, the differential form can avoid the input impedance to be impacted by the undesired bond wire inductance  $L_{BW}$ . The differential input impedance seen between the gates doesn't contain the real value created by  $L_{BW}$  and parasitic gate capacitors  $C_{gs,1p}$  and  $C_{gs,1n}$ , otherwise the passive gain of the voltage-boosting network will be reduced. The load of the LNA is two resonant networks consisting of  $L_{Lp}$  ( $L_{Ln}$ ) and  $C_{Lp}$  ( $C_{Ln}$ ), isolated from the input voltage-boosting network by cascodes  $M_{2p}$  and  $M_{2n}$ .

The voltage boosting network consists of a resistance  $R_A$ , an inductance  $L_A$  and the overall capacitance at the input.  $C_v$  is a capacitance tank controlled by a tuning loop, to be shown later in this section.  $C_{rec}$  is the input capacitance of the rectifier.  $C_{g,p}$  and  $C_{g,n}$  are the isolation capacitors to separate the DC bias of the LNA and the DC voltage of the rectifier. Since the effective passive gain at the gate of  $M_{1p}$  ( $M_{1n}$ ) is reduced by a capacitive voltage divider formed by  $C_{g,p}$  ( $C_{g,n}$ ) and  $C_{gs,1p}$  ( $C_{gs,1n}$ ),  $C_{g,p}$  ( $C_{g,n}$ ) should be much higher than  $C_{gs,1p}$  ( $C_{gs,1n}$ ).

As explained in section II, the high voltage-gain provided by the voltage-boosting network relaxes the gain requirement of the LNA and significantly improves the NF, thereby reducing the power consumption considerably. Moreover, the size of

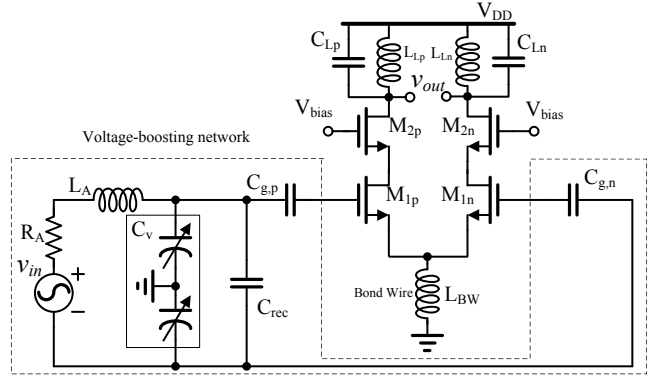


Fig. 5: LNA circuit with proposed OM interface. The bias circuitry is not shown.

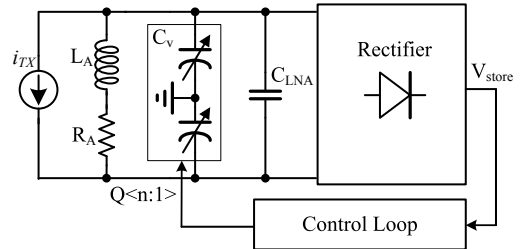


Fig. 6: Proposed OM interface with control loop.

the input transistors can be quite small since the limited current flowing through them, thus only introducing a little gate resistance noise.

#### B. Control Loop

One issue of the proposed interface that deserves attention is its sensitivity to impedance mismatch, which is mainly caused by the environment variations. A control loop to compensate the impedance variations in the voltage-boosting antenna-rectifier interface has been introduced in [1]. An interesting fact is that both the proposed interface and the antenna-rectifier interface in [1] operate at resonance. Thus, the control loop is used in the proposed interface and shared between the energy harvester and LNA, as shown in Fig. 6.

In the antenna-rectifier interface [1], the control loop is designed to maximize the voltage on storage capacitor  $V_{store}$  by detecting the slope of  $V_{store}$  and then adjusting the capacitance  $C_v$  at the interface. In other words, the resonance frequency  $f_r = 1/2\pi\sqrt{L_A C_A}$  is tuned to the frequency of the input signal with highest power rather than a center frequency desired by the LNA. Thus, the transmitter in the system, represented by  $i_{TX}$  in Fig. 6, is utilized to replace the antenna signal  $v_{in}$  as the input signal since the frequency of  $i_{TX}$  is the desired frequency of the system  $f_c$ . The resonance frequency  $f_r$  is tuned to  $f_c \sqrt{1 + 1/Q_A^2}$ , approximately equal to  $f_c$  when  $Q_A$  is quite high. Another benefit we obtain from this control loop is that a part of the power used in the tuning procedure is saved by the storage capacitor rather than being dissipated completely by the antenna resistance  $R_A$ .

### C. Rectifier and Antenna

We used the same rectifier and antenna introduced in [1]. The antenna is a high Q inductive antenna with an impedance around  $X_{L_A} = 713\Omega$  and  $10\Omega \leq R_A \leq 20\Omega$  at 915MHz. The rectifier features a  $V_{TH}$  self-cancelation technique.

### IV. SIMULATION RESULTS

The LNA with the proposed OM interface has been designed at circuit level and verified with simulations in AMS 0.18 $\mu\text{m}$  technology. The antenna impedance is set to be  $R_A = 20\Omega$  and  $X_{L_A} = 713\Omega$ , i.e. the quality factor of the voltage-boosting network  $Q_{in,OM}$  is 36. Tuning capacitors  $C_v$  and rectifier input capacitance  $C_{rec}$  are binary scaled from 4-256fF and about 120fF respectively. The sizes of  $M_{1p}$ ,  $M_{2p}$ ,  $M_{1n}$  and  $M_{2n}$  are all 5 $\mu\text{m}/0.18\mu\text{m}$ . In order to be much greater than the parasitic gate capacitances of the transistors,  $C_{g,p}$  and  $C_{g,n}$  are set to be 1pF. The load inductance  $L_{Lp}$  is assumed to be 40nH with a 5.3 $\Omega$  parasitic resistance, providing an impedance of 10k $\Omega$  at resonance. Note that the assumed quality factor of the load inductance might be too high to be a practical value, but it's still reasonable since the performance improvement gained from this high quality factor inductive load will not be taken into account in the performance comparison. The current of each branch is 25 $\mu\text{A}$ , yielding a total power consumption of 50 $\mu\text{W}$  at 1V power supply.

The simulation results are compared with another LNA design based on the 50 $\Omega$  PM interface shown in Fig. 3a to show how much performance improvement we can achieve from the proposed interface. This LNA is also in a differential form, and has the same isolation transistors ( $M_{2p}$  and  $M_{2n}$ ) and inductive loads as the proposed design. The inductance  $L_t = L_g + 2L_s$  is equal to  $L_A$ , and  $L_s$  is chosen so as to create a differential resistance  $2L_s\omega_T = R_{A,50} = 50\Omega$ , thus yielding a quality factor of the input passive network  $Q_{in,PM} = (R_A/2R_{A,50})Q_{in,OM} = 7.2$ . One extra capacitance is added in parallel with the parasitic gate capacitances to resonate with  $L_t$ .

The simulated differential to single-ended gains of the two LNAs are shown in Fig. 7. At the center frequency  $f_c = 915\text{MHz}$ , the proposed OM interface offers 12.3dB higher voltage gain than the 50 $\Omega$  PM LNA. This is slightly less than the expected value  $20\log(R_A/2R_{A,50}) = 14\text{dB}$  indicated by Eq. (4) since  $Q_{in,OM}$  is decreased slightly by the gate resistances of  $M_{1p}$  and  $M_{1n}$ . Fig. 7 also shows that the LNA with an OM interface has a 1.8dB lower NF. Fig. 8 shows that voltage gain and NF are degraded by an increase of the antenna resistance  $R_A$  due to the lowering of the passive gain at the interface.

### V. CONCLUSION

An optimally mismatched (OM) interface and an LNA based on this interface for EHSNs have been presented. It has been shown that an LNA with the proposed OM interface has 12.3dB better voltage gain and 1.8dB lower NF than an LNA with the 50 $\Omega$  PM interface. Moreover, the sensitivity of the energy harvester is also enhanced by the high voltage boosting

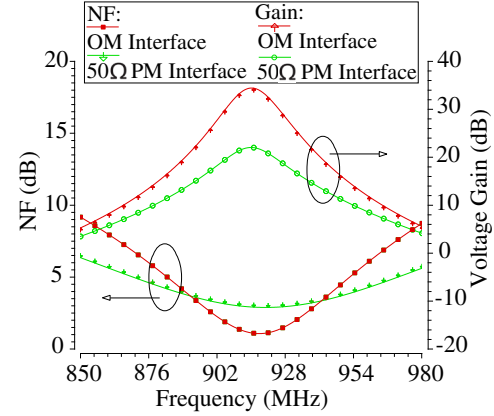


Fig. 7: Voltage gain and NF comparison for LNAs with an OM interface and a 50 $\Omega$  PM interface.

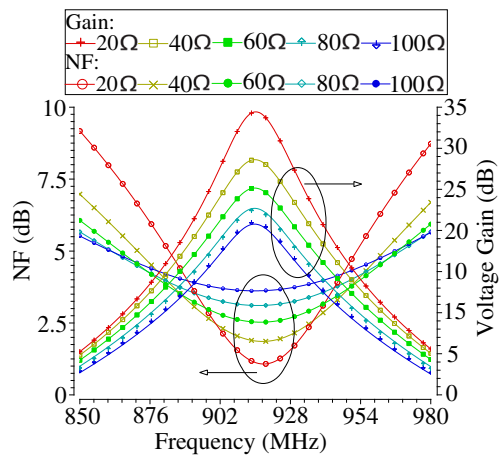


Fig. 8: Effect of antenna resistance  $R_A$  on the voltage gain and NF of the LNA with an OM interface.

of the OM interface. Thus, the proposed OM interface and LNA can serve as a good candidate for use in EHSNs.

### REFERENCES

- [1] M. Stoopman, W. A. Serdijn, and K. Philips, "A robust and large range optimally mismatched rf energy harvester with resonance control loop," in *Circuits and Systems, 2012. ISCAS '12. Proceedings of the 2012 International Symposium on*, vol. 5, may 2004, pp. V-213 – V-216 Vol.5.
- [2] T. Le, K. Mayaram, and T. Fiez, "Efficient far-field radio frequency energy harvesting for passively powered sensor networks," *Solid-State Circuits, IEEE Journal of*, vol. 43, no. 5, pp. 1287 –1302, may 2008.
- [3] N. Roberts and D. Wentzloff, "A 98nw wake-up radio for wireless body area networks," in *Radio Frequency Integrated Circuits Symposium (RFIC), 2012 IEEE*, june 2012, pp. 373 –376.
- [4] J. Pandey and B. Otis, "A sub-100 $\mu\text{w}$  mics/ism band transmitter based on injection-locking and frequency multiplication," *Solid-State Circuits, IEEE Journal of*, vol. 46, no. 5, pp. 1049 –1058, may 2011.
- [5] F. Zhang, Y. Zhang, J. Silver, Y. Shakhshir, M. Nagaraju, A. Klinefelter, J. Pandey, J. Boley, E. Carlson, A. Shrivastava, B. Otis, and B. Calhoun, "A batteryless 19 uw mics/ism-band energy harvesting body area sensor node soc," in *Solid-State Circuits Conference Digest of Technical Papers (ISSCC), 2012 IEEE International*, feb. 2012, pp. 298 –300.
- [6] B. Razavi, *RF Microelectronics*, ser. Prentice Hall Communications Engineering and Emerging Technologies, 2011.